Effect of Floating Vegetation on Wind Flow and Wave in Closed Water Body

Ozaki, Akinori
International Plant Form for Asian Agricultural Education, Faculty of Agriculture, Kyushu University, Assistant Professor

Mori, Ken
Laboratory of Bioproduction and Environment Information Sciences, Division of Bioproduction and Environment Information Sciences, Department of Bioproduction and Environmental Sciences, Faculty of Agriculture, Kyushu University

Hirai, Yasumaru
Laboratory of Bioproduction and Environment Information Sciences, Division of Bioproduction and Environment Information Sciences, Department of Bioproduction and Environmental Sciences, Faculty of Agriculture, Kyushu University

Hamagami, Kunihiko
Laboratory of Bioproduction and Environment Information Sciences, Division of Bioproduction and Environment Information Sciences, Department of Bioproduction and Environmental Sciences, Faculty of Agriculture, Kyushu University, Research

https://doi.org/10.5109/16136

出版情報：九州大学大学院農学研究院紀要. 54 (2), pp.489-498, 2009-10-29. Faculty of Agriculture, Kyushu University
バージョン：
権利関係：

J. Fac. Agr., Kyushu Univ., **54** (2), 489–498 (2009)

Effect of Floating Vegetation on Wind Flow and Wave in Closed Water Body

Akinori OZAKI[1]*, Ken MORI[2], Yasumaru HIRAI[2] and Kunihiko HAMAGAMI[3]

Laboratory of Bioproduction and Environment Information Sciences, Division of Bioproduction and Environment Information Sciences, Department of Bioproduction and Environmental Science, Faculty of Agriculture, Kyushu University, Fukuoka 812–8581, Japan
(*Received June 29, 2009 and accepted July 13, 2009*)

When we address a water quality problem in some closed water bodies, it is very important to solve the relationship between the disturbances and flow. Turbulent and convective flows may be induced by mechanical and thermal disturbances, respectively. Disturbances induce the circulation flow of water environmental substance and the water quality depends on this circulation. It is considered that when a mechanical disturbance act on the water surface, the generation of turbulent energy at the water surface and its transportation to the lower layers affects the circulation flow of the water environmental substances. In addition due to the mechanical disturbances act on the water surface, we cannot disregard the effect of the luxuriant growth of floating vegetation and it is conjectured that the impact of disturbances will depend on luxuriant rate of floating vegetation. Therefore, it is important to clarify the effect of luxuriant growth of floating vegetation on the impact of disturbances generated by wind shear.

In this study, we particularly focus attention on the mechanical disturbance induced by wind in the closed water body, and we experimentally elucidate the characteristics of the wind flow and wind wave in a closed water body with floating vegetation by using a test tank. The results indicated that the energy of the wind flow was attenuated by the presence of floating vegetation and the attenuation of the energy of the wind wave increased with the coverage of floating vegetation. This attenuation effect was expressed using a resistance coefficient and wave characteristics.

INTRODUCTION

In some closed water bodies, fluids are generally stratified by their vertical density difference (temperature, dissolved oxygen, nutrient salts, etc.). This density difference arises due to limited inflow and outflow in closed water bodies. In the absence of disturbance in these water bodies, the vertical density stratification is stabilized. With the action of the wind on the surface of such closed water bodies, surface layer becomes turbulent due to the wind current. Such wind action in closed water bodies with density stratification gives rise to the entrainment phenomenon at the density interface. This phenomenon, which results from the mixing of the upper and lower water layers, lowers the density interface and then affects the water quality of the closed water body. A previous study on the entrainment phenomenon reported that this phenomenon was dominated by the turbulent energy that induces entrainment and stability of density stratification (Mori *et al.*, 1989b). This turbulent energy can be expressed as the entrainment coefficient $E=u_e/u_{*a}$, where u_e is the entrainment velocity and u_{*a} is the air friction speed. The stability of density stratification can be expressed as an over–all Richardson number $R_{ia}=\Delta\rho gh/\rho_a u_{*a}^2$, where $\Delta\rho_0$ is the difference in density between the upper and lower layers, h_1 is the water depth of the upper layer. With regard to the entrainment phenomenon of wind–induced flow, Wu. (1973), Kit *et al.* (1980) and Mori *et al.* (1989a) explained the relation between the Richardson number and the ratio of the potential energy of wind–induced flow at the water surface to work by wind action, and they also reported that the entrainment velocity in the density stratification depended on the turbulent structure near the density interface that was induced by strong turbulence due to wind action. This means that the transportation of turbulent energy at the air–water interface is important to intermix the stratified flow. A previous study on the transportation of turbulent energy at the air–water interface reported that in a test tank experiment, when wind acts on the water surface, the velocity of the water surface reduces with the increase in fetch length (Wu, 1975).

As mentioned above, for closed water bodies, if the water quality variation or hydrodynamics are considered, the effect of the wind flow and wind wave are one of the most important concepts for water flow dynamics. In particular when we expect the floating vegetation in a small–scale closed water body to absorb nutrient salts, it is also important to clarify the effect of the growing conditions of this vegetation on mechanical disturbance.

Our previous study (Ozaki *et al.*, 2004), on the wind–induced entrainment phenomenon with floating vegetation, reported that when the surface of a closed water body is partially covered with floating vegetation, the entrainment velocity based on wind–induced flow decreases

[1] International Plat Form for Asian Agricultural Education, Faculty of Agriculture Kyushu University, Assistant Professor
[2] Laboratory of Bioproduction and Environmental Information Sciences, Division of Bioproduction and Environment Sciences, Department of Bioproduction Environmental Sciences, Faculty of Agriculture Kyushu University
[3] Laboratory of Bioproduction and Environmental Information Sciences, Division of Bioproduction and Environment Sciences, Department of Bioproduction Environmental Sciences, Faculty of Agriculture Kyushu University, Research Fellow of JSPS.
* Corresponding author (E–mail: a–ozaki@agr.kyushu–u.ac.jp)

with the increase in the coverage of vegetation. Further, we reported that these changes occurred because the plants decreased the amount of turbulent flow energy produced by the wind–induced flow, followed by a reduction in the vertical mixing capability. However, the transportation mechanism of turbulent energy at the air–water interface has not been clarified. Thus, it is important to clarify the effect of floating vegetation on the transportation mechanism of turbulent energy at the air–water interface in a closed water body. As mentioned above we have experimentally considered the characteristics of wind flow and wind waves in a closed water body with floating vegetation.

METHODS AND DATA

Previous study of wind–induced entrainment phenomenon in closed water body with floating vegetation

Fig. 1 shows our previous experimental results (Ozaki *et al.*, 2004) of the wind–induced entrainment phenomenon in a closed water body with floating vegetation by using the wind tunnel test tank shown in Fig. 2. A two–layered, stratified density flow was created in the test tank. The upper layer comprised fresh water, while the lower layer comprised salt water. The vegetation conditions are shown in Fig. 3. In this experiment, we measured the lowering rate of the density interface accompanying the constant power of wind blowing and defined the entrainment velocity. In Fig. 1, over–all Richardson number R_{ia} and entrainment coefficient E are plotted on the horizontal and vertical axes, respectively. We defined these values as follows:

$$R_{ia} = \Delta\rho g h / \rho_a U_{*a}^2 \quad (1)$$

$$E = U_e / U_{*a} \quad (2)$$

where $\Delta\rho$ is the density difference between the upper and lower layers; h, the initial water depth of the upper layers; ρ_a, the density of air; U_{*a}, the air friction velocity; U_e, the entrainment velocity; and g, the acceleration of gravity. As seen in Fig. 1, the entrainment coefficient E in the experiment with floating vegetation was considerably smaller than that in the experiment without floating vegetation. Further, the larger the coverage rate of the floating vegetation, the lower the entrainment velocity. In other words, these results show that the vertical mixing capability inside a water body is attenuated with an increase in the coverage rate of the floating vegetation. In this

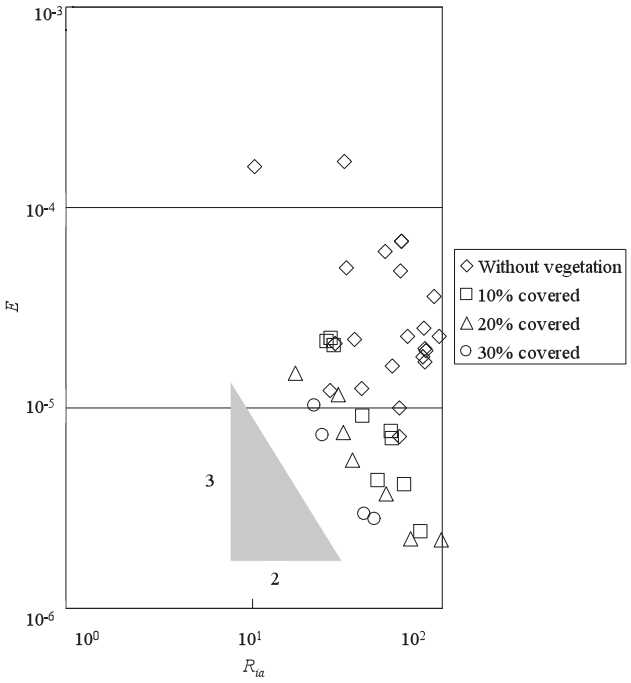

Fig. 1. Relation between R_{ia} and E obtained previous study.

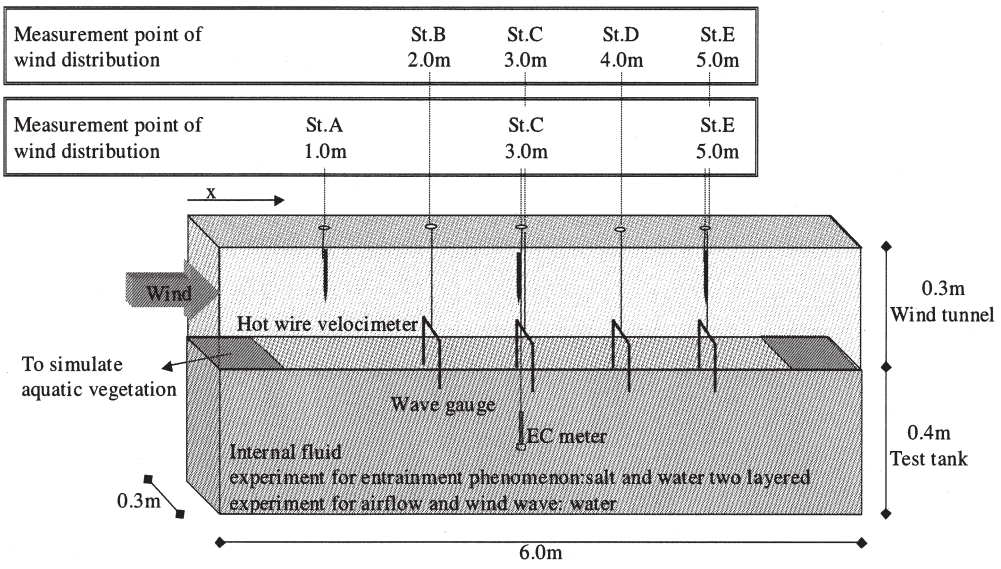

Fig. 2. Schematic diagram of experiment apparatus.

study, in order to verify this conclusion in detail, we experimentally considered the effect of floating vegetation on the turbulence of the surface layer that is induced by the wind flow and wind wave, which is closely related to the entrainment phenomenon.

Experimental method of wind flow and wind wave

The test tank was made of acrylic plate (length=6 m, width=0.3 m, depth=0.4 m). The wind tunnel comprised a piece of block–board placed on the test tank (length=6 m, width=0.3 m, depth=0.3 m) (cf. Fig. 2). The test tank was filled with fresh water. Wind in the wind tunnel was generated by an air blower. The blowing power was increased gradually at a specified wind velocity. The following values were measured: vertical wind velocity distribution, air temperature, water temperature and wave profiles. The wind velocity was measured with a hot–wire velocimeter, water and air temperature with a thermocouple and wave profiles with a resistance wire wave gauge in which two platinum wires were strained. The sampling time for the wave profiles was 120 s, and the sampling frequency was 100 Hz. The experimental conditions for wave profile measurement are listed in Table 1. In these tables, $U_{0.15}$ denotes the representative wind velocity measured at 3.0 m from the windward side and a height of 0.15 m from the water surface. The wind velocity distribution and temperature were measured at 3 points: 1 m (St A), 3 m (St C) and 5 m (St E) from the windward side. The wave profiles were measured at 4 points: 2 m (St B), 3 m, 4 m (St D) and 5 m from the windward side. Instead of using floating vegetation, we used floating vegetation made from polystyrene foam plates. The plate section had a thickness of 3 mm. We placed the simulated vegetation at both ends of the test tank. The setting conditions are shown in Fig. 3.

RESULTS

Wind flow on water surface

Wind distribution and air friction velocity

In order to clarify the effect of floating vegetation on the development of wind flow, we measured wind velocity distributions at each measurement point and characteristics of wind. Fig. 4 shows the wind velocity distributions that were measured at St C for various conditions of floating vegetation. It has previously been reported that wind distribution near the water surface complies with a logarithmic low (Shemdin, 1972), (Wu, 1975); our results are in agreement with this finding. In addition, with an increase in the wind velocity, the velocity gradient near the water surface increased. These results indicated that the turbulent boundary layer of the wind wave at the water surface is similar to the wall boundary layer. As a consequence, it was possible to draw a regression line in these figures and calculate the air friction velocity using the following equation.

$$U(z) / U_{*a} = (1 / \kappa) \ln (z / z_0), \qquad (3)$$

where $U(z)$ is the wind velocity at a height z; U_{*a} the air friction velocity; κ the Karman constant; z the height from the water surface; and z_0 the roughness constant. Fig. 5 shows the relation between the calculated air friction velocity and the wind velocity at a height of 10 m above the water surface, U_{10}. Additionally U_{10} was calculated using a regression expression. In the case of St A, there was little difference between the vegetation conditions; however, in the case of St C and St E, the air friction velocity decreases slightly with an increase in the coverage rate of floating vegetation. It is considered that this phenomenon occurs due to obstruction of the wind flow by floating vegetation, thereby causing a decrease in

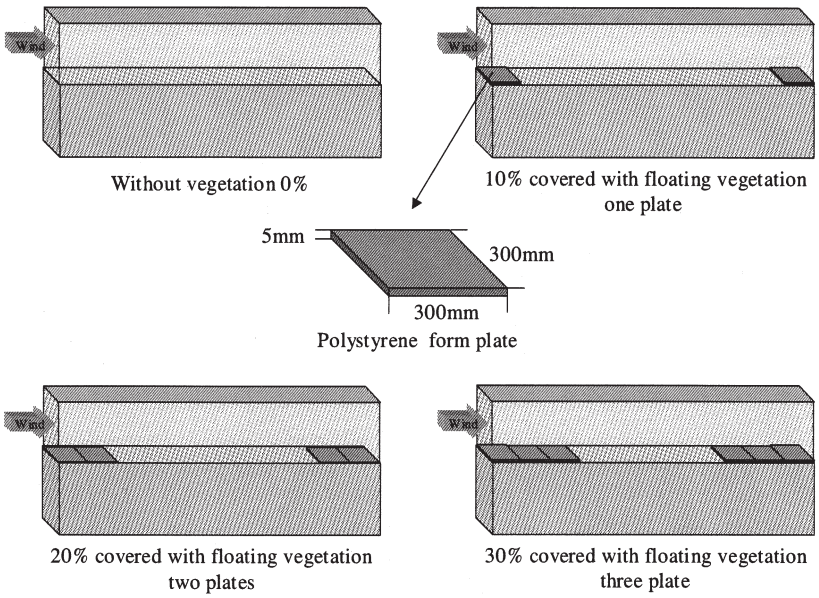

Fig. 3. Conditions simulating surface coverage by simulated floating vegetation.

Table 1. Experimental conditions for wind wave profiles

Coverage rate of floating vegetation	Measurement point	Wind velocity $U0.15$ (m/s)	Air temperature (°C)	Coverage rate of floating vegetation	Measurement point	Wind velocity $U0.15$ (m/s)	Air temperature (°C)
Without vegetation 0–division	St. B, D	2.20	20.7	20% covered	St. B, D	2.23	22.1
	St. A, C	2.22	20.1		St. A, C	2.21	23.4
	St. B, D	2.73	20.8		St. B, D	2.69	22.1
	St. A, C	2.67	20.3		St. A, C	2.66	23.4
	St. B, D	3.28	20.8		St. B, D	3.28	22.0
	St. A, C	3.29	20.8		St. A, C	3.36	23.4
	St. B, D	3.77	20.9		St. B, D	3.76	21.9
	St. A, C	3.74	21.0		St. A, C	3.80	23.5
	St. B, D	4.29	20.9		St. B, D	4.27	22.0
	St. A, C	4.19	21.2		St. A, C	4.14	23.6
	St. B, D	4.74	21.0		St. B, D	4.67	22.1
	St. A, C	4.70	21.4		St. A, C	4.72	23.8
	St. B, D	5.23	21.0		St. B, D	5.18	22.1
	St. A, C	5.14	21.6		St. A, C	5.17	23.9
	St. B, D	5.69	21.3		St. B, D	5.58	22.2
	St. A, C	5.58	21.8		St. A, C	5.67	24.0
	St. B, D	6.18	21.5		St. B, D	6.03	22.3
	St. A, C	6.12	21.9		St. A, C	6.12	24.2
	St. B, D	6.70	21.7		St. B, D	6.59	22.4
	St. A, C	6.55	22.2		St. A, C	6.68	24.4
10% covered	St. B, D	2.26	21.5	30% covered	St. B, D	2.24	22.2
	St. A, C	2.28	22.3		St. A, C	2.30	24.4
	St. B, D	2.64	21.6		St. B, D	2.59	22.1
	St. A, C	2.61	22.3		St. A, C	2.75	24.4
	St. B, D	3.30	21.6		St. B, D	3.22	22.0
	St. A, C	3.36	22.3		St. A, C	3.29	24.4
	St. B, D	3.74	21.6		St. B, D	3.79	22.0
	St. A, C	3.78	22.4		St. A, C	3.70	24.5
	St. B, D	4.19	21.8		St. B, D	4.21	22.0
	St. A, C	4.24	22.6		St. A, C	4.16	24.6
	St. B, D	4.72	21.8		St. B, D	4.68	22.0
	St. A, C	4.70	22.7		St. A, C	4.69	24.7
	St. B, D	5.17	21.9		St. B, D	5.14	22.0
	St. A, C	5.23	22.9		St. A, C	5.13	24.8
	St. B, D	5.69	22.0		St. B, D	5.61	22.1
	St. A, C	5.71	23.0		St. A, C	5.50	25.1
	St. B, D	6.12	22.2		St. B, D	6.06	22.1
	St. A, C	6.10	23.2		St. A, C	6.07	25.2
	St. B, D	6.75	22.4		St. B, D	6.64	22.2
	St. A, C	6.62	23.2		St. A, C	6.64	25.3

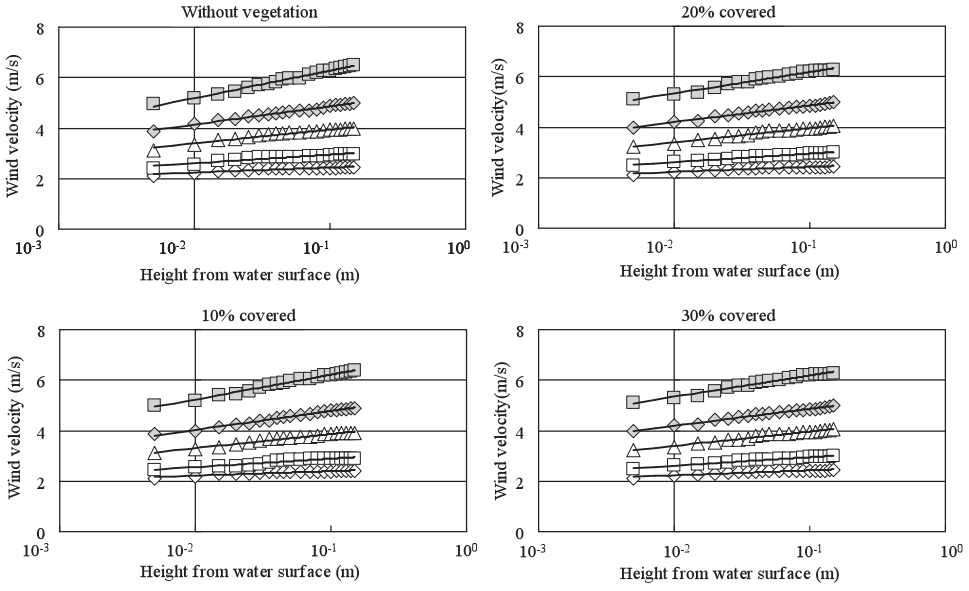

Fig. 4. Wind velocity distribution at St C for various conditions of floating vegetation.

its energy, and the decrease in the shearing stress with an increase in plant coverage.

Resistance coefficient for various conditions of floating vegetation

Generally, the vertical transportation of momentum at the water surface is equal to the shear stress, which acts on the water surface. This transportation is important from with the viewpoint of engineering problems, such as the development of the wind flow and wind wave. The shear stress, which acts on the water surface, can be expressed as follows in relation to the wind velocity at a height of 10 m above the water surface (Tsuruya, 1983).

$$\tau_a = \rho_a C_d U_{10}^2 \tag{4}$$

or

$$C_d = \left(\frac{U_{*a}}{U_{10}}\right)^2 \tag{5}$$

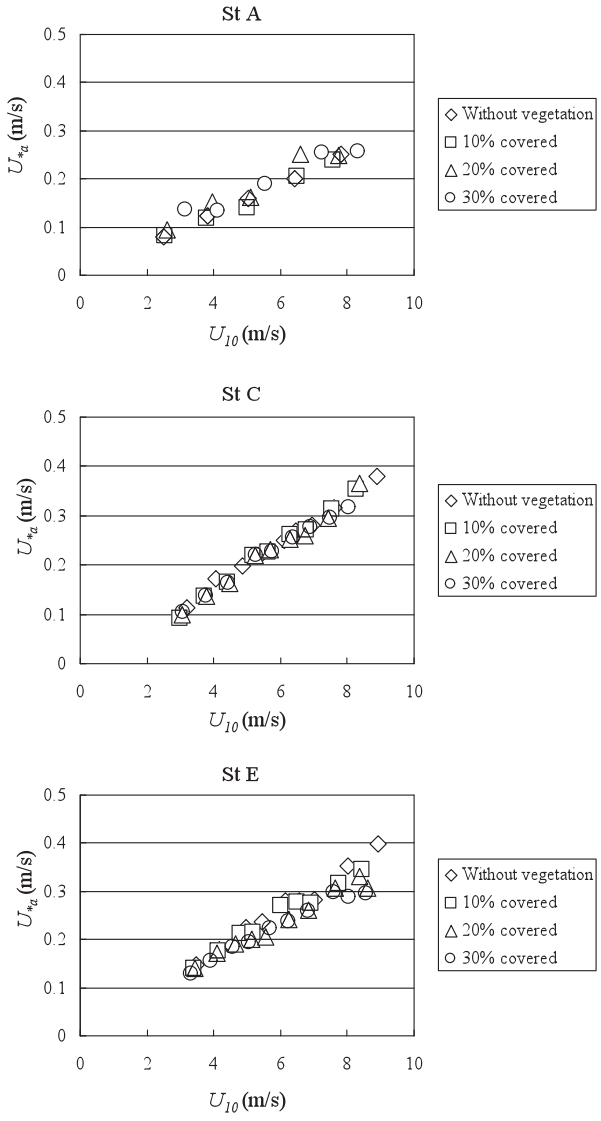

Fig. 5. Relation between calculated air friction velocity and representative wind velocity.

where ρ_a is the density of air.

This method is referred to as the bulk method. Although this method is usually employed when considering the wind flow in the ocean, since its formula is easy to derive and considerable number of experimental results can be obtained by using it. Fig. 6 shows the relation between the resistance coefficients and representative wind velocity for various conditions of floating vegetation. These figures include the experimental results obtained by Honda and Mitsuyasu (1980) and Amorocho and DeVeries (1980). From these figures it is evident that our resistance coefficient is smaller than the value obtained by Honda. On the other hand, our value was slightly larger than that obtained by Amorocho and DeVeries. These differences were considered to be result of the differences in the experimental conditions. Our resistance coefficients had the same value regardless of the value of representative wind velocity. Hence, we used an averaged resistance coefficient for discussion in this study. Fig. 7 shows this averaged resistance coefficient for various conditions of floating vegetation. In this figure, the value means the ratio of resistance coefficient to in the case with no vegetation. Kraus and Turner (1967) reported that when U_{10} ranges from 3 m/s to 16 m/s, the averaged resistance coefficient ranges from 1.27×10^{-3} to 1.33×10^{-3}. Our resistance coefficients were slightly larger than those defined by Kraus and Turner. These differences are considered to be due to the difference in experimental conditions between researchers such as length of fetch or scale of test tank. However, our results indicated the qualitative differences of floating vegetation; the resistance coefficient tended to decrease with the increase in the coverage rate of the floating vegetation. Further, this tendency was observed to be strong in the leeward side.

As mentioned above, we can conclude that the resistance encountered by air differs between the vegetation

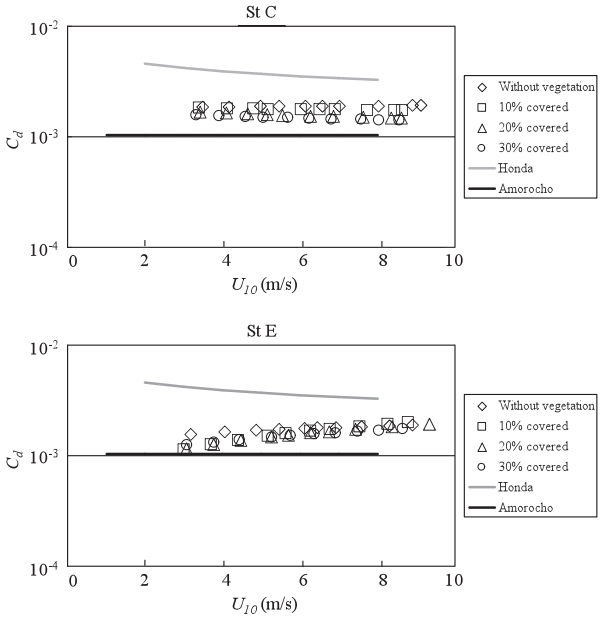

Fig. 6. Relation between resistance coefficient and representative wind velocity.

and the water surface. In other words, since the vegetation was simulated using polystyrene foam plates in this study, in terms of the resistance characteristics, the vegetation was considered to be a smooth region due to which encountered comparatively lower degree of resistance and passed smoothly. On the other hand, the water surface was considered to be a rough region due to which the wind experienced resistance from the water surface.

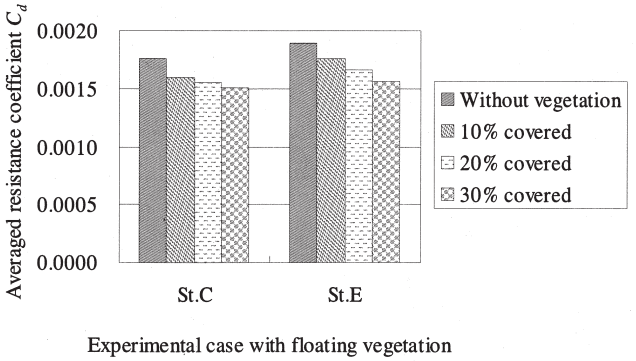

Fig. 7. Averaged resistance coefficient for various conditions of floating vegetation.

Wind wave characteristics

Validation of wave profiles

From the experimental results of wind flow on the water surface, it was clarified that the luxuriant growth of floating vegetation changed the resistance characteristics of the water surface. It is considered that these changes affect the development of wind waves and development of wind–induced flow in turn. Therefore, it is important to clarify the characteristics of the wind wave when considering the wind–induced entrainment. In this regard, we clarified the effect of floating vegetation on the development of wind waves.

First, we calculated the wind–wave distribution by using the measurements of the wave profiles. The statistical characteristics of wind waves in the laboratory have been studied by many researchers (Tokuda and Toba, 1981; Tokuda and Toba, 1982; Goda, 1983, etc). Wave height distribution and power spectrum distribution are the generally used statistical characteristics of waves. In this study, we used these two statistical characteristics for verifying the wind wave that was obtained in the experiment. It was previously reported (Longuet–Higgins, 1952) that a well developed wave height distribution, complies with the Rayleigh distribution, i.e. the probability density function can be expressed by the following equation;

$$p\left(\frac{H}{\bar{H}}\right) = \frac{\pi}{2}\frac{H}{\bar{H}^2}\exp\left\{-\frac{\pi}{4}\left(\frac{H}{\bar{H}}\right)^2\right\}, \qquad (6)$$

where H is the wave height; $\bar{H}$, the averaged wave height; and $p\left(\frac{H}{\bar{H}}\right)$, the probability density function. This equation represents the probability that the wave height ranges from H to $H+dH$ is $P\ (H / \bar{H}) \cdot dH$. In addition, this equation assumes that the waveform is symmetrical for a vertical to averaged water level and the group wave consists of a narrow–band frequency wave. Fig. 8 shows an example of the calculated results of the wave height distribution measured at St C. In these figures, the line shows the calculated result using Eq (6), while the bar shows the measurement result of the wave height distribution. These figures show that the calculated wave height distributions are in agreement with the Rayleigh distribution for each measurement point and experimental case. The probability density exists for a value within three times the averaged wave height. Similarly the calculated results with Rayleigh distribution for other experimental conditions of floating vegetation, and they show the same tendency. Therefore, from the analytical result of the wave height distribution, it can be stated that the waveform data obtained in these experiments appropriately represent the waves.

Next, we analyzed wave profiles by using spectral analysis. For the spectrum calculation, we first divided the acquired data into 2048 data blocks; the data were initially calculated using FFT and then by using the ensemble average of FFT result. With regard to the form of the power spectrum, it has been reported that the spectrum analysis result for a well developed wave complies with the following equation that was proposed by Phillips, for high frequencies.

$$\phi\ (f) = \beta g^2 f^{-5} \qquad (7)$$

where $\phi\ (f)$ is the power spectrum; g, the acceleration of gravity; f, the frequency; and β, a constant. Burling had proposed that $\beta = 0.951\times10^{-5}$. Fig. 9 shows an example of the calculated results. Our calculated result did not comply with this equation for high frequencies at St B. This can be explained by the fact that the wave was in an early stage of development and was too small to be measured with our wave gauge. The same reasons can cite for the experimental case wherein the representative wind velocity is below 4.0 m/s. Therefore, from the analytical results of the power spectrum of the wind wave, it can be stated that the waveform data obtained for St B and the experimental case for a representative wind velocity of below 4.0 m/s were not suitable wave representations. On the other hand, for St C, St D, St E and the experimental case in which the representative wind velocity is above 4.0 m/s, the calculated result complied with this equation. In the experimental case with a representative wind velocity of 4.7 m/s, β showed the highest agreement, and when the value of representative wind velocity increased beyond 4.7 m/s, β tended to increase. Furthermore, as the representative wind velocity and the fetch increased, the peak of the power spectrum shifts to the low frequency for all conditions of vegetation. The power spectrum values also decreased with an increase in the coverage rate. These results imply that the increase in the wind velocity and fetch length has the same effect on the development of a spectrum and the peak of the power spectrum shifts to the low frequency side with the development of the spectrum. In comparison of the results of the experimental

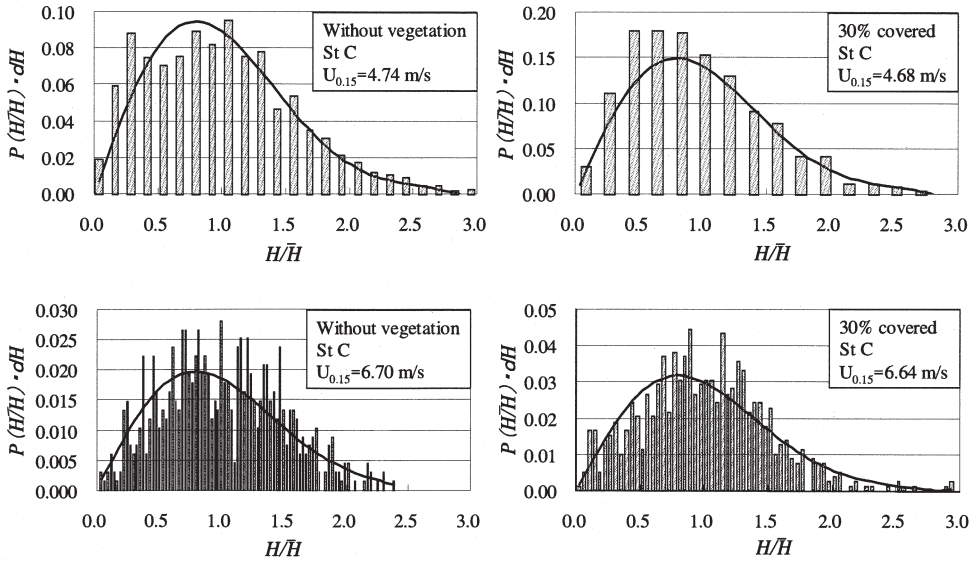

Fig. 8. Wave height distribution measured at St C experimental case 0% and 30% covered with floating vegetation.

case without vegetation and that with 30% coverage of floating vegetation, the power spectrum for the latter case revealed a clearly low value and the development rate of the wind wave was low. Therefore, it was considered that the luxuriant growth of floating vegetation reduced the wind energy and inhibited the development of the wind wave.

Significant wave height and wave period

Based on the above analytical result, we calculated the significant wave height and significant wave period at each measurement point using the zero–up–crossing method. Before considering the representative wind wave, we need to verify whether the wave profiles in this experiment were obtained in a steady. For this purpose, we calculated the significant wave height and significant wave period at intervals of 20 s for various conditions of floating vegetation. Fig. 10 and Fig. 11 show the calculated results for the significant wave height and significant wave period at intervals of 20 s. From these figures, the significant wave height was almost changeless with time. However, the significant wave period was slightly changeful with time. The reason of changefulness was considered that the wave profiles which obtained immediately after the measurement start was in development stage. It is thought that the wave of development stage should not be put into consideration. So we used the date which obtained 60 sec after from measurement start for calculate significant wave height and significant wind wave. Fig. 12 and Fig. 13 show the calculated results of the significant wave height and significant wave period at each measurement point. From the figures the significant wave height and significant wave period were attenuated with increase in the coverage of the floating vegetation, and this tendency became prominent as the wind velocity increased. Therefore, the presence of floating vegetation affects not only the shearing of the wind energy but also the growth of the wind wave.

DISCUSSION

In order to clarify the effect of floating vegetation on wind flow and wind wave in a closed water body, we carried out experiments by using a test tank and with simulated floating vegetation.

From the experimental results of wind flow on a water surface, it is evident that the presence of abundant floating vegetation changed the conditions of the water surface on the windward side. In other words, since the vegetation in this study was simulated with polystyrene foam plates, the vegetation was considered to be a smooth region due to which encountered a comparatively lower degree of resistance and passed smoothly. On the other hand, the water surface was considered to be a rough region due to which the wind encountered resistance from the water surface. It is evident that these effects originated due to the use of polystyrene foam plates as a method of simulating vegetation in this study. It is considered that natural vegetation present in actual environments dose offer resistance to the passage of wind. Therefore, it is necessary to improve the method of simulating vegetation, so that the artificial material is more representative of actual vegetation. However, it could be verified that a luxuriant growth of floating vegetation changes the resistance characteristics of the wind flow on a water surface.

The experimental results for the wind wave and the validity of the measured wave profiles, which was determined from the analysis of these profiles, showed that the calculated wave height distribution in the present experiment agreed with the Rayleigh distribution for all the measurement points and experimental cases. From these results it can be stated that the all the waveform data obtained in these experiments appropriately represented the waves. However, an analysis of the wave profiles by

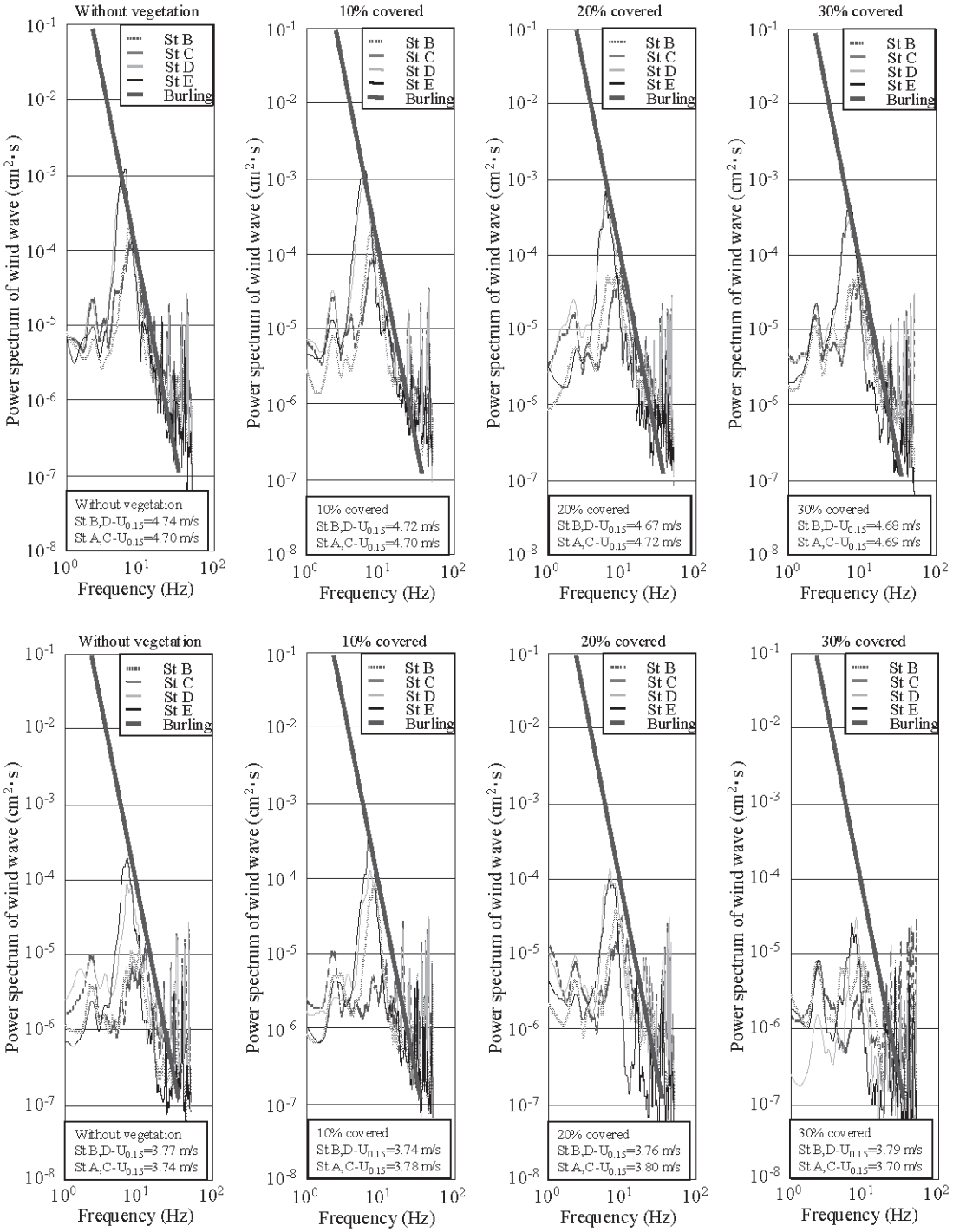

Fig. 9. Power spectrum distribution for various conditions of floating vegetation.

the power spectrum of the wind wave revealed that the distribution of the power spectrum obtained at St B and the experimental case in which the representative wind velocity was below 4.0 m/s was not in agreement with the previous theoretical equation. From these results, it is clear that the waveform data obtained in two cases were not appropriate wave representation. Therefore, when considering the effect of floating vegetation on a wind wave by using a wind tunnel test tank, the power spectrum method is the preferred verification method to assess the validity of the wind wave.

In addition, the analytical result of the power spectrum showed that as the wind velocity and the fetch length increased, the peak of the power spectrum shifted to low frequency side. This indicated that the wave was developed with an increase in the wind velocity and fetch length. Further, the power spectrum value decreased as the coverage rate of vegetation increased. This indicates that the presence of abundant floating vegetation reduces the wind energy and inhibits the development of a wind wave.

Consequently, the significant wave height and the significant wave period were attenuated with an increase in the coverage rate of floating vegetation, as shown by

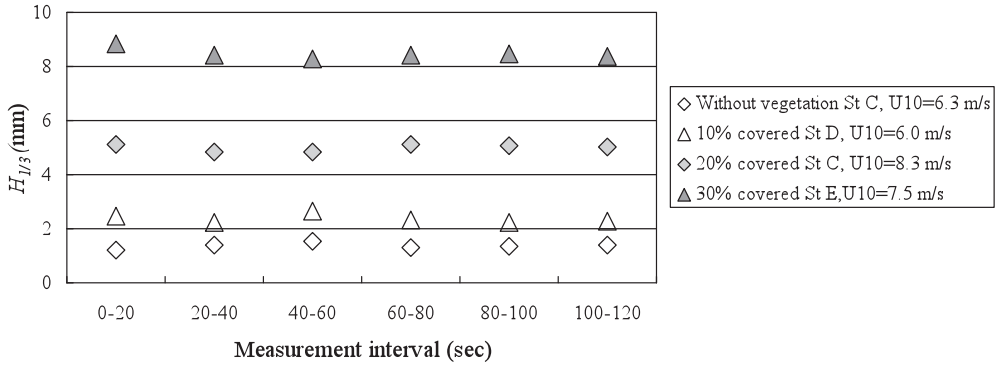

Fig. 10. Significant wave height calculated at intervals of 20 sec for various conditions of floating vegetation.

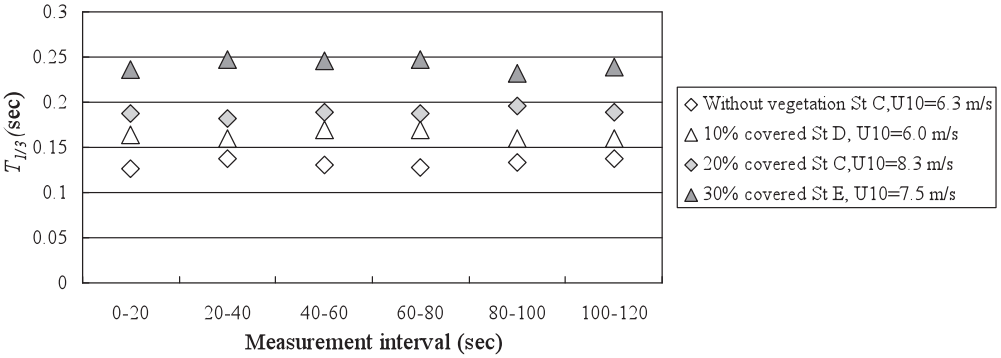

Fig. 11. Significant wave period calculated at intervals of 20 sec for various conditions of floating vegetation.

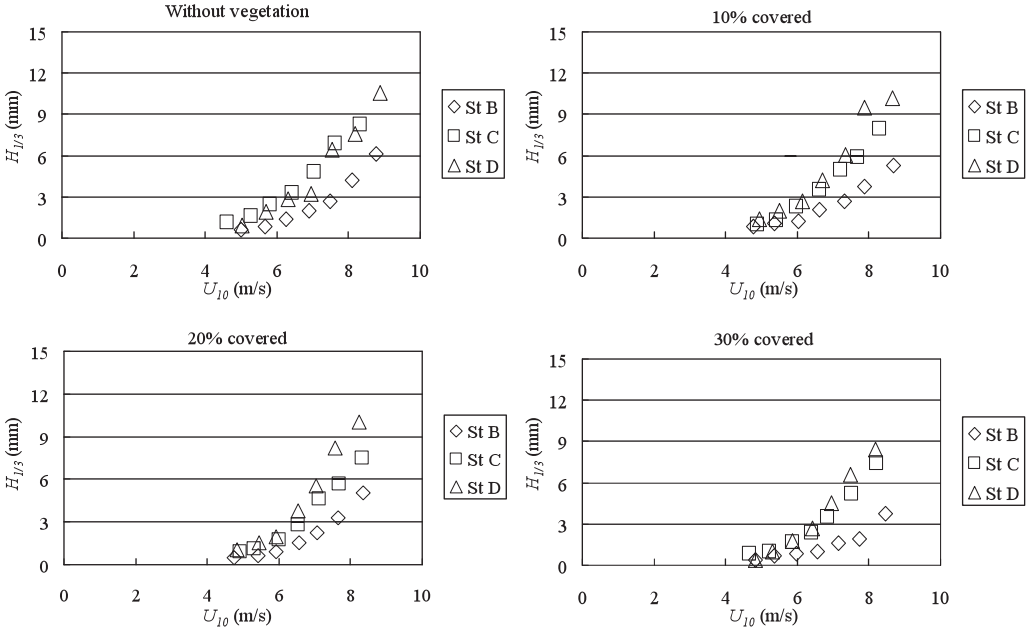

Fig. 12. Relation between significant wave height and wind velocity at 10 m above water surface for various conditions of floating vegetation.

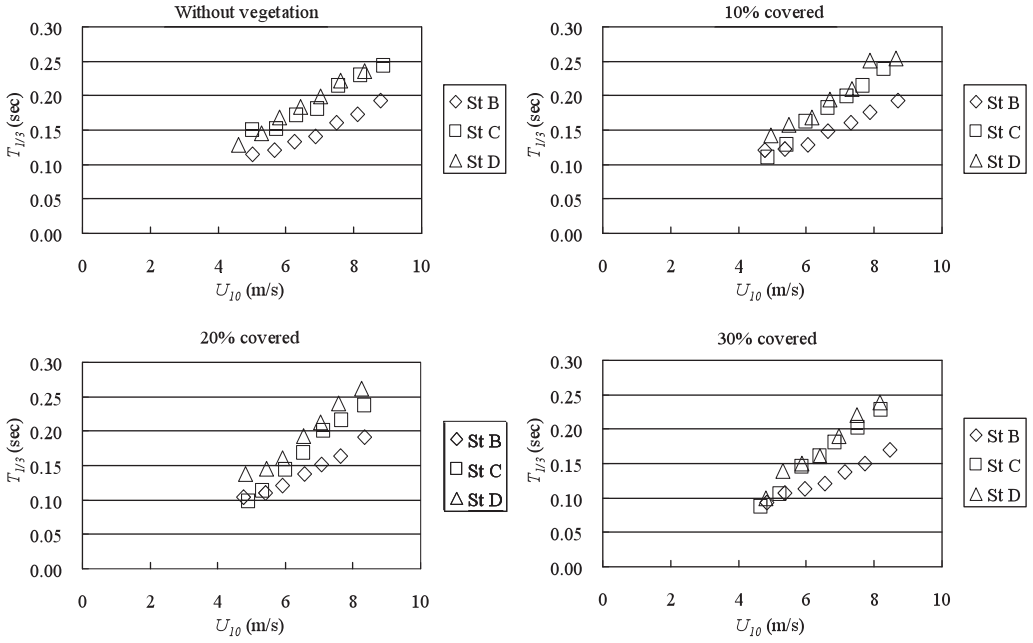

Fig. 13. Relation between significant wave period and wind velocity at 10 m above water surface for various conditions of floating vegetation.

the experimental results for these significant wave heights and the significant wave period.

From the above explanation of the effect of floating vegetation on a wind wave, it is clear that when abundant vegetation is present on the windward side, it can change the fetch length and inhibit the development of a wind wave. This mechanism can impact the generation of turbulent energy at the water surface and the circulation flow of the water environmental substances. Therefore, a clarification of whole mechanisms between air– water interfaces will be future task in this study.

REFERENCE

Amorocho, J., De Veries. J. J 1980 A New Evaluation of the Wind Stress Coefficient over Water Surfaces. *Journal of Geophysical Research*,. **85**(C1): 433–442

Goda, Y. 1983 A Unified Nonlinearity Parameter of Water Waves, *Report of The Port and Harbour Research Institute*. **22**(3): 30

Honda, T., Mitsuyasu, H. 1980 Experimental Research of Effect of Wind on Water Surface (In Japanese). *Proceedings of Coastal Engineering*. **27**: 90–93

Kit, E., Berent, E., Vajda, M. 1980 Vertical Mixing Induced by Wind and a Rotating Screen in a Stratified Fluid in a Channel, *Journal of Hydraulic Research*. **18**: 35–58

Kraus, E. B., Turner, J. S. 1967 A One–Dimensional Model of the Seasonal Thermocline, Ⅱ. *The general theory and its consequences*. Tellus, **19**: 98–106

Longuet–Higgins, M. S. 1952 On the Statistical Distribution of the Heights of Sea Waves, *Journal of Marine Reserch*. **9**(3): 245–266

Mori, K., Tohara, Y., Kato O. 1989a Experimental Research of Entrainment Rate of Density Interface due to a Wind Induced Current (In Japanese with English Abstract). *Transaction of the Japanese Society of Irrigation, Drainage and Reclamation Engineering*. **144**: 85–93

Mori, K., Tohara, Y., Shikasyo, S., Hiramatsu, K., Kato, O., Cho, H 1989b Turbulent Structure of Wind Induced Two–Layer Flow (In Japanese with English Abstract). *Transaction of the Japanese Society of Irrigation, Drainage and Reclamation Engineering*. **144**: 75–84

Ozaki, A., Mori, K., Inoue, E., Haraguchi, T. 2004 Impact of aquatic plants on entrainment phenomena based on wind–induced flow in a closed density stratified water area, *Journal of the International Society of Paddy and Water Environment Engineering*. **2**: 125–134

Shemdin, O. H. 1972 Wind–Generated Current and Phase Speed of Wind Waves. *Journal of Physical Ocean*. **2**: 411–419

Tokuda, M., Toba, Y 1981 Statistical Characteristics of Individual Waves in Laboratory Wind Waves Ⅰ. Self–Consistent Similarity Regime. *Journal of the Oceanographical Society of Japan*. **37**: 243–258

Tokuda, M., Toba, Y 1982 Statistical Characteristics of Individual Waves in Laboratory Wind Waves Ⅱ. Self–Consistent Similarity Regime. *Journal of the Oceanographical Society of Japan*. **38**: 8–14

Tsuruya, H. 1983 Experimental Study of Wind Driven Currents in a Wind–Wave Tank –Effect of Return Flow on Wind Driven Currents–. *Report of the Port and Harbor Research Institute*, **22**(2): 128–174

Wu, J. 1973 Wind–Induced Turbulent Entrainment Across a Stable Density Interface. *Journal of Fluid Mechanics*. **61**: 275–287

Wu, J. 1975 Wind–Induced Drift Currents. *Journal of Fluid Mechanics*. **68**: 49–70